Scientific Research Publishing

Open Journal of Applied Sciences, 2026, 16(5), 1854-1870
https://www.scirp.org/journal/ojapps
ISSN Online: 2165-3925
ISSN Print: 2165-3917

UWB Localization Algorithm Based on BiLSTM and Bahdanau Attention

Guanhui Li, Guoliang Wei, Zhuang Xi

School of Optical-Electrical Computer Engineering, University of Shanghai for Science and Technology, Shanghai, China
Email: l475gh@163.com

How to cite this paper: Li, G.H., Wei, G.L. and Xi, Z. (2026) UWB Localization Algorithm Based on BiLSTM and Bahdanau Attention. *Open Journal of Applied Sciences*, **16**, 1854-1870.
https://doi.org/10.4236/ojapps.2026.165103

Received: April 20, 2026
Accepted: May 24, 2026
Published: May 27, 2026

Copyright © 2026 by author(s) and Scientific Research Publishing Inc.
This work is licensed under the Creative Commons Attribution International License (CC BY 4.0).
http://creativecommons.org/licenses/by/4.0/

Open Access

Abstract

Ultra Wide Band (UWB) technology has a wide range of applications in indoor positioning due to its high precision and strong anti-interference ability. However, in complex indoor environments, UWB signals are susceptible to multipath effects and non line of sight conditions, leading to a decrease in positioning accuracy. A UWB high-precision positioning algorithm based on Bidirectional Long Short Term Memory (BiLSTM) network and Bahdanau attention is proposed to address this issue. By using BiLSTM network to deeply model the temporal dependence of TOA observation sequence, and embedding Bahdanau attention mechanism, adaptive weight allocation is implemented on the feature information of UWB signal to highlight the contribution of key features to the positioning results. The experimental results show that the proposed algorithm can effectively suppress the interference caused by NLOS, ultimately achieving an average positioning error of 6.7 cm. Compared with UWB positioning algorithms based on Recurrent Neural Network (RNN), LSTM, and Gated Recurrent Unit (GRU), the positioning errors are reduced by 40.71%, 37.15%, and 37.79%, respectively. The experimental results show that the deep learning model combining BiLSTM and Bahdanau attention mechanism has higher robustness and localization accuracy in complex environments.

Keywords

Ultra-Wide Band, Non-Line-of-Sight, Bidirectional Long Short-Term Memory Network, Bahdanau Attention Mechanism

1. Introduction

In indoor environments, the Global Positioning System (GPS) is obstructed by buildings and cannot perform effective positioning. In contrast, ultra wideband

technology has become an ideal choice for indoor positioning due to its advantages such as high precision, strong penetration, and good resistance to multipath and interference [1]. UWB is a wireless communication technology with a bandwidth greater than 500 MHz, which can provide high-resolution positioning services over short distances and maintain good performance in multi obstacle environments. Due to its excellent positioning accuracy and reliability, UWB performs well in indoor positioning applications and is widely used in fields such as smart homes and logistics tracking. At present, common methods for UWB positioning include Time of Arrival (TOA) [2], Time Difference of Arrival [3], Angle of Arrival [4], and Received Signal Strength Indication [5]. Among them, TOA algorithm has become the mainstream method for UWB positioning due to its low power consumption, low cost, and stable and reliable operation characteristics.

In indoor environments, the ranging error of UWB positioning is mainly affected by multipath effects [6], multiple access interference [7], clock synchronization errors [8], and Non Line of Sight (NLOS) errors [9]. Existing research has explored various methods to improve UWB positioning accuracy, covering the application of technologies such as inertial measurement units [10], Wi Fi [11], Kalman filtering [12], and multi-sensor fusion [13]. In addition, deep learning methods are widely used to improve localization accuracy. For example, reference [14] proposed a Feedforward Neural Network (FNN) method for Line of Sight (LOS) and Non Line of Sight (NLOS) recognition, which can effectively alleviate the negative impact of confined space and various obstacles on localization. Reference [15] combines UWB technology and Convolutional Neural Networks (CNN) positioning method to estimate the transmitter position through RGB images, improving indoor positioning accuracy and robustness. Reference [16] proposed a deep learning model based on LSTM, which effectively improves indoor positioning accuracy by using UWB TOA distance data to predict user location. Reference [17] proposes a UWB positioning method based on spatiotemporal attention graph neural network, which improves the ability to capture geometric relationships through multi label ranging modeling and exhibits higher positioning accuracy and robustness in non line of sight environments. Reference [18] proposed an attention based UWB ranging error compensation algorithm, which improves the accuracy of UWB ranging by re evaluating the importance of channel characteristics.

Although existing research has significantly improved the accuracy of UWB indoor positioning systems, there is still room for further optimization of positioning accuracy. To this end, this article proposes a new UWB indoor positioning method that combines bidirectional gated recurrent unit BiLSTM with Bahdanau attention mechanism. BiLSTM has advantages in processing temporal data and can effectively capture the dynamic characteristics of UWB signals, while Bahdanau attention mechanism enhances the model's focus on key signal features by dynamically assigning weights. The combination of the two enables the model to

extract and process UWB signal features more accurately in complex environments, effectively improving indoor positioning accuracy and reducing positioning errors. The experimental results show that the proposed model significantly improves the accuracy of UWB indoor positioning and effectively reduces positioning errors.

2. UWB Positioning Method

The traditional UWB indoor positioning method commonly uses TOA positioning method for position estimation. TOA positioning method is a distance measurement method that calculates the signal propagation distance by measuring the propagation time from the transmitter to the receiver. In UWB communication, due to the extremely wide signal bandwidth, the short pulses of UWB signals can be well distinguished in space, thereby accurately measuring the time when the signal arrives at the receiver. The basic principle of TOA positioning method is to determine the distance between the transmitter and receiver by measuring the time difference between the arrival of the transmitted signal at the receiver. Specifically, when the transmitted signal originates from the source and travels through a certain propagation path to reach the receiver, the clock signal inside the receiver will record the time of signal arrival. The distance of signal propagation can be calculated based on the known signal propagation speed and the time difference between the transmitted signal and the clock signal of the receiver.

The physical essence of TOA positioning method lies in accurately observing the pulse propagation delay between the tested node and each reference station, and then obtaining the spatial Euclidean distance between the two points. With the extremely high time resolution unique to UWB signals, the receiving end can accurately capture the rising edge of nanosecond pulses, achieving high-precision measurement of signal transmission time. Based on this, the trilateration (TRI) [19] method is used to reverse solve the geometric coordinates of the target entity, as shown in Figure 1.

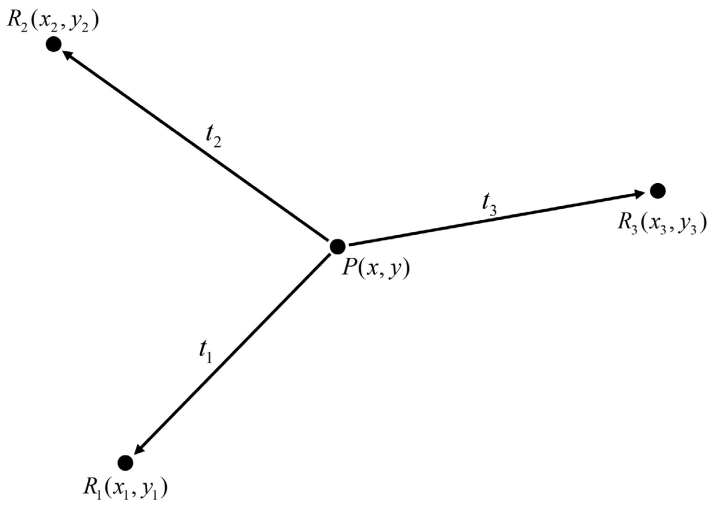

Figure 1. Principle diagram of TOA-based localization method.

After obtaining the distance from the unknown tag to the positioning base station, the traditional UWB indoor positioning system uses the trilateration method to calculate the specific location of the unknown tag. However, in practical situations, due to multipath effects, multiple access interference, clock synchronization errors, and non line of sight errors, the final result calculated by the trilateration method is often only an approximate value. The logical core of TRI positioning mechanism is to construct a set of nonlinear equations in two-dimensional or three-dimensional space by obtaining the distance information between three or more observation starting points and unknown targets. From a geometric perspective, this method essentially solves the geometric intersection positions of multiple circular rings or spheres with each base station as the center and observation distance as the radius. Figure 2 illustrates the basic principle of TRI positioning technology.

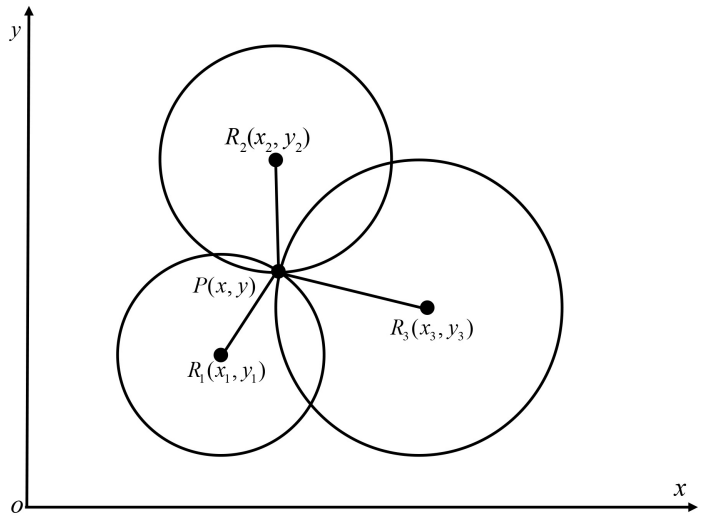

Figure 2. Trilateration principle diagram.

The distance d_i between the UWB unknown tag $P(x,y)$ and the positioning base station $R_i(x_i,y_i)$ is represented as:

$$d_i^2 = (x_i - x)^2 + (y_i - y)^2 \tag{1}$$

The values of i are 1, 2, and 3. By expanding Equation (1), we obtain:

$$d_i^2 = x_i^2 + x^2 - 2x_i x + y_i^2 + y^2 - 2y_i y \tag{2}$$

Considering $i = k$, Equation (2) can be written as:

$$d_k^2 = x_k^2 + x^2 - 2x_k x + y_k^2 + y^2 - 2y_k y \tag{3}$$

By subtracting Equation (3) from Equation (2), we can obtain:

$$d_i^2 - d_k^2 + x_k^2 + y_k^2 - x_i^2 - y_i^2 = 2(x_k - x_i)x + 2(y_k - y_i)y \tag{4}$$

Considering $i = 1$ and variable exponent $k = 2, 3$, can obtain:

$$\begin{bmatrix} 2(x_2 - x_1) & 2(y_2 - y_1) \\ 2(x_3 - x_1) & 2(y_3 - y_1) \end{bmatrix} \begin{bmatrix} x \\ y \end{bmatrix} = \begin{bmatrix} d_1^2 - d_2^2 + x_2^2 + y_2^2 - x_1^2 - y_1^2 \\ d_1^2 - d_3^2 + x_3^2 + y_3^2 - x_1^2 - y_1^2 \end{bmatrix} \tag{5}$$

By solving the above equation system, the coordinates of the unknown UWB tag can be obtained. Equation (5) can be viewed as $Ax = b$, representing the values of A, x, and b for a system of linear equations:

$$A = \begin{bmatrix} 2(x_2 - x_1) & 2(y_2 - y_1) \\ 2(x_3 - x_1) & 2(y_3 - y_1) \end{bmatrix} \tag{6}$$

$$x = \begin{bmatrix} x \\ y \end{bmatrix} \tag{7}$$

$$b = \begin{bmatrix} d_1^2 - d_2^2 + x_2^2 + y_2^2 - x_1^2 - y_1^2 \\ d_1^2 - d_3^2 + x_3^2 + y_3^2 - x_1^2 - y_1^2 \end{bmatrix} \tag{8}$$

The solution of a system of linear equations should minimize the following definition of δ:

$$\delta = (Ax - b)^{\mathrm{T}} (Ax - b) \tag{9}$$

$$x = \begin{bmatrix} x & y \end{bmatrix}^{\mathrm{T}} \tag{10}$$

By using the minimum mean square error (MMSE) method, x can be solved as:

$$x = \left(A^{\mathrm{T}} A\right)^{\mathrm{T}} A^{\mathrm{T}} b \tag{11}$$

3. Model Architecture

3.1. Bidirectional Long Short Term Memory Network

When dealing with sequence observations with long-range dependency characteristics, conventional RNNs are prone to the computational dilemma of gradient decay or explosion, which severely limits their ability to capture macroscopic historical patterns. To overcome this bottleneck, researchers have designed an LSTM architecture. As shown in Figure 3, LSTM covers three major control hubs: forgetting, input, and output, giving the network the powerful ability to automatically screen and remember long-term spatiotemporal correlations.

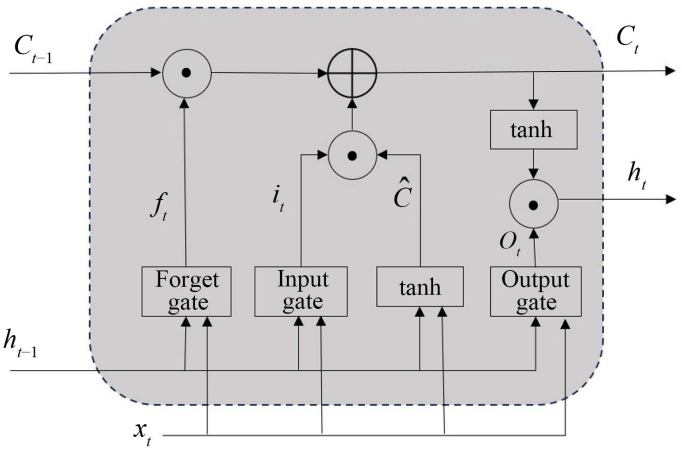

Figure 3. Long short-term memory network structure.

At time step t, the input gate first computes the gating coefficient based on the current input vector $\boldsymbol{x}_t$ and the hidden state from the previous time step $\boldsymbol{h}_{t-1}$. The expression is given as follows:

$$\boldsymbol{f}_t = \sigma\left(\boldsymbol{W}_f\left[\boldsymbol{h}_{t-1}, \boldsymbol{x}_t\right] + \boldsymbol{b}_f\right) \tag{12}$$

here σ denotes the sigmoid activation function, $\boldsymbol{W}_f$ represents the weight matrix, and $\boldsymbol{b}_f$ is the bias vector. The output of the forget gate determines the proportion of information retained from the previous cell state $\boldsymbol{C}_{t-1}$.

The input gate is responsible for incorporating new input features, and its computation can be expressed as:

$$\boldsymbol{i}_t = \sigma\left(\boldsymbol{W}_i\left[\boldsymbol{h}_{t-1}, \boldsymbol{x}_t\right] + \boldsymbol{b}_i\right) \tag{13}$$

The candidate cell state is obtained through a nonlinear transformation, which can be expressed as:

$$\hat{\boldsymbol{C}} = \tanh\left(\boldsymbol{W}_c\left[\boldsymbol{h}_{t-1}, \boldsymbol{x}_t\right] + \boldsymbol{b}_c\right) \tag{14}$$

where $\boldsymbol{W}_i$ and $\boldsymbol{W}_c$ denote the weight matrices of the input gate and the candidate state, respectively, and $\boldsymbol{b}_i$ and $\boldsymbol{b}_c$ are the corresponding bias terms. The candidate cell state $\hat{\boldsymbol{C}}$ is used to store newly extracted feature information at the current time step.

By jointly considering the regulatory effects of the forget gate and the input gate, the cell state at the current time step is updated as:

$$\boldsymbol{C}_t = \boldsymbol{f}_t \odot \boldsymbol{C}_{t-1} + \boldsymbol{i}_t \odot \hat{\boldsymbol{C}} \tag{15}$$

where $\odot$ denotes the element-wise multiplication operation.

Finally, the output gate is employed to control the influence of the cell state on the hidden layer output, and its computation is given by:

$$\boldsymbol{o}_t = \sigma\left(\boldsymbol{W}_o\left[\boldsymbol{h}_{t-1}, \boldsymbol{x}_t\right] + \boldsymbol{b}_o\right) \tag{16}$$

The corresponding hidden state output is given by:

$$\boldsymbol{h}_{t-1} = \boldsymbol{o}_t \odot \tanh\left(\boldsymbol{C}_t\right) \tag{17}$$

The BiLSTM model developed on this basis further raises the ceiling of time-series data analysis. As shown in **Figure 4**, unlike the inherent mode of traditional LSTM that can only deduce forward along the time series in one direction, BiLSTM synchronously adds a reverse parsing link. This dual track parallel computing logic enables the network to inherit historical residual memory and perceive future rehearsal states in advance at any time node, thereby constructing a global sequence dependency graph without blind spots.

BiLSTM consists of two LSTM sub networks with identical structures but independent parameters. Among them, one LSTM processes the input sequence in positive chronological order to extract temporal information from the past to the current time; The other model the sequence in reverse chronological order, backtracking from the future to the current moment to supplement contextual information. Finally, at the same time step, the outputs of forward and backward LSTM

are concatenated or fused to obtain a feature representation that contains both temporal information before and after.

Overall, as an extended form of LSTM, BiLSTM further enhances the modeling ability of the model for sequential data by introducing bidirectional information flow, making it more stable and efficient in dealing with complex temporal problems. Specifically in the UWB positioning task, by applying it to the modeling of TOA ranging sequences and introducing a bidirectional structure, the bidirectional dependencies in the ranging data can be more fully explored, thereby more accurately characterizing the time delay shifts and distortions caused by factors such as occlusion. This not only enhances the model's ability to represent abnormal signals but also provides a more reliable feature foundation for subsequent weight allocation by attention mechanisms, ultimately helping to reduce positioning errors.

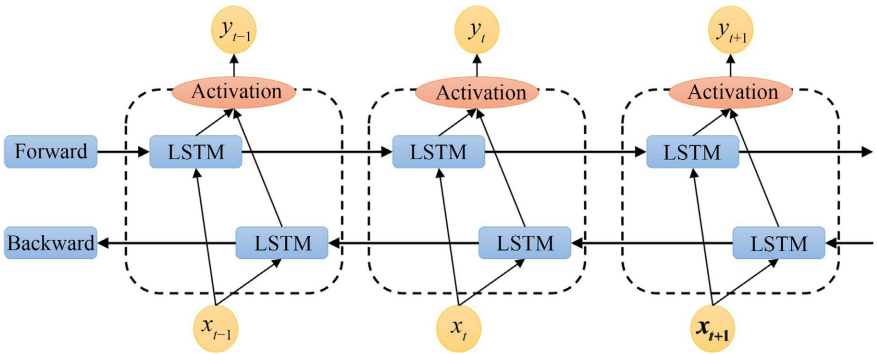

Figure 4. Schematic diagram of BiLSTM structure.

3.2. Bahdanau Attention Mechanism

In the UWB positioning process, due to the susceptibility of signal propagation to multipath effects and NLOS environment, the role of TOA data corresponding to different time steps in positioning calculation is not consistent. Some time point information is more critical, while others may contain more noise or redundant information. Based on this characteristic, the Bahdanau attention mechanism is introduced to model the importance of each time step feature, thereby achieving adaptive enhancement of key information.

As shown in **Figure 5**, from an implementation perspective, the Bahdanau attention mechanism evaluates the features of each time step in the TOA sequence one by one, and dynamically calculates the corresponding weight coefficients based on the hidden state at the current time. That is to say, when the model performs feature fusion, it does not treat information from all time steps equally, but instead weights them differentially based on their contribution to the current task, so that more discriminative features receive higher attention.

The introduction of this mechanism enables BiLSTM to focus more on effective information when processing TOA sequences, while weakening the influence of noise or interference data, thereby improving the overall quality of feature extrac-

tion. The core lies in the calculation process of attention weights, which combines the current hidden state with the output features of all time steps to generate corresponding attention scores, and then completes weighted summation based on this to obtain a more representative representation of contextual information.

In the calculation process, the current hidden state is first concatenated with the outputs of each time step, and mapped to the feature space through linear transformation. Then, the activation function tanh is input for nonlinear transformation to obtain the attention score:

$$e_{i,t} = \boldsymbol{v}_a^{\mathrm{T}} \cdot \tanh\left(\boldsymbol{W}_a \cdot \left[\boldsymbol{h}_i; \boldsymbol{s}_{t-1}\right] + \boldsymbol{b}_a\right) \tag{18}$$

$$\alpha_{i,t} = \frac{\exp\left(e_{i,t}\right)}{\sum_{k=1}^{T} \exp\left(e_{k,t}\right)} \tag{19}$$

In the formula, $\boldsymbol{v}_a$ denotes the trainable parameter vector, and $\boldsymbol{b}_a$ represents the bias term. All attention scores are normalized using the softmax function to obtain the corresponding attention weights $\alpha_{i,t}$, which reflect the importance of each time-step feature to the current output.

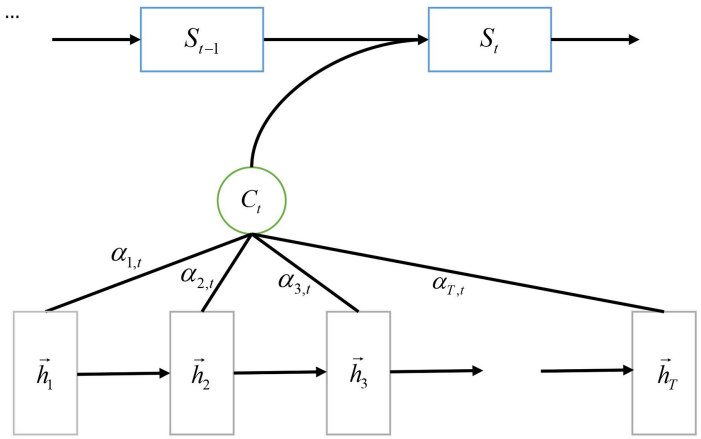

Figure 5. Bahdanau attention mechanism.

After obtaining the normalized attention weights $\alpha_{i,t}$, a weighted sum is performed on the outputs of the TOA sequence to construct the context vector $\boldsymbol{c}_t$. This vector aggregates key information in the time series and plays a critical role in the prediction at the current time step. The calculation process is expressed as:

$$\boldsymbol{c}_t = \sum_{i=1}^{T} \alpha_{i,t} \boldsymbol{h}_i \tag{20}$$

where $\boldsymbol{h}_i$ denotes the hidden state at the i-th time step, and T is the sequence length. Through the weighted sum operation, information from different time steps is integrated into the context representation according to their importance.

At the output stage of the model, the context vector c_t is fused with the current hidden state to provide richer feature information for the final output. Leveraging this weight assignment-based mechanism, the BiLSTM-Bahdanau model can more

effectively highlight key temporal features in complex NLOS environments, thereby improving the overall accuracy and stability of UWB indoor positioning.

3.3. Algorithm Steps

The detailed algorithm steps of the BiLSTM model integrated with the Bahdanau attention mechanism for processing UWB Time-of-Arrival (TOA) data are as follows:

Input: TOA data received by UWB base stations

Output: Predicted target position coordinates generated by the model

Step 1: Data Preprocessing

Collect TOA data from the UWB system and the corresponding base station coordinates, ensuring the completeness and accuracy of the data. Integrate the TOA data and base station coordinates into a format suitable for model input, and standardize the input features to eliminate scale differences between different features, thereby ensuring the effectiveness and convergence speed of model training. No additional outlier removal or synchronization correction was performed on the data.

Step 2: Model Construction

Build a BiLSTM network and introduce the Bahdanau attention mechanism, which dynamically assigns attention weights by calculating the correlation between the hidden state and each time step in the input sequence. Based on the output of the attention mechanism, design fully connected layers to generate the final predicted position coordinates.

Step 3: Model Training and Evaluation

Continuously adjust parameters to determine the optimal configuration of the model, and validate the model's fitting ability on the test set.

Through the above steps, the BiLSTM model combined with the Bahdanau attention mechanism can effectively process UWB TOA data, improve indoor positioning accuracy, and exhibit strong robustness in complex multipath and non-line-of-sight (NLOS) environments.

4. Experiments and Result Analysis

4.1. Model Training and Parameter Selection

The experimental operating system is Windows 11, with a system memory of 16 GB, and a server environment equipped with an NVIDIA GeForce RTX 3050 GPU. The deep learning framework used is PyTorch 2.5.0. To verify the effectiveness of the proposed model, the dataset used in the experiments in this paper is derived from Reference [20]. In this dataset, four positioning base stations are deployed within a 6.5 m × 2.5 m experimental area, with coordinates (0 m, 0 m), (6.5 m, 0 m), (6.5 m, 2.5 m), and (0 m, 2.5 m), respectively. During the experiment, a mobile anchor moves along a predefined trajectory within the experimental area to simulate a moving target in practical application scenarios. Positioning data are collected synchronously using an ultra-wideband (UWB) system and a motion capture system to ensure data consistency and synchronization.

The dataset contains 3200 samples, each including four distance values and the

corresponding x and y coordinates of the mobile anchor. In the experiment, the dataset was divided into an 80% training set and a 20% testing set. The selection of model parameters was based on comparative experiments involving different parameter configurations conducted on the training set. The BiLSTM model combined with the Bahdanau attention mechanism uses four input neurons to receive the four distance values of the mobile anchor and two output neurons to predict the x and y positions of the mobile anchor. Since each sample in the adopted dataset is an independent observation rather than continuous time series data, no sliding window or time step expansion method was employed when inputting each sample into the BiLSTM model.

This paper analyzes the variation of the loss value of the BiLSTM model with the Bahdanau attention mechanism as a function of the number of training epochs from multiple aspects, including learning rate, optimizer, batch size, number of hidden neurons, number of BiLSTM network layers, and loss function.

First, the influence of different learning rates on model performance is analyzed. A large learning rate often leads to unstable training, while a small learning rate may result in slow convergence or even failure to train the model. As shown in Figure 6, when the learning rate is set to 0.01, the model achieves both a favorable convergence speed and good stability. Therefore, a learning rate of 0.01 is selected for the proposed model.

Next, the influence of different optimizers on model performance is analyzed. Optimizers play a crucial role in improving model accuracy. When deep neural networks are employed for positioning, the neural network may suffer from vanishing gradients or exploding gradients as energy propagates through network layers. These problems become more severe with increasing network complexity, thereby degrading network performance. To avoid the issues of vanishing gradients and exploding gradients, it is critical to select an appropriate optimizer. As shown in Figure 7, the model converges rapidly and steadily when the Nadam optimizer is adopted. Therefore, the Nadam optimizer is chosen for the proposed model.

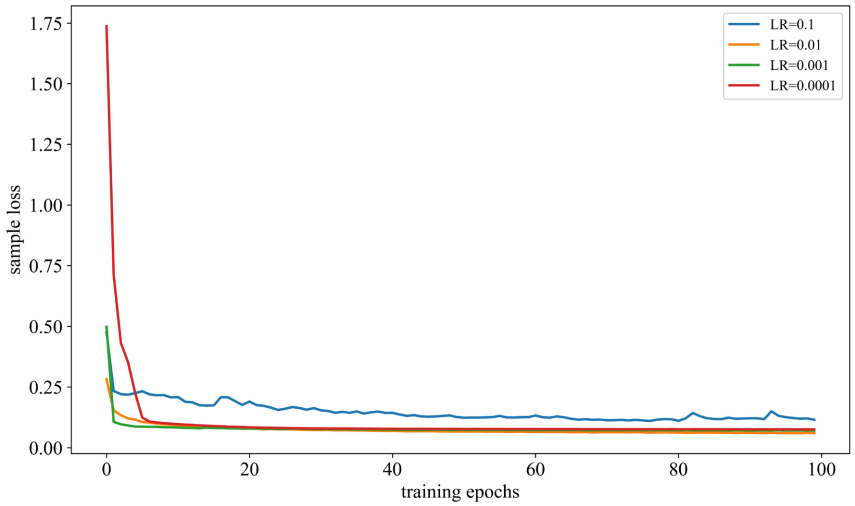

Figure 6. Training loss curves at different learning rates.

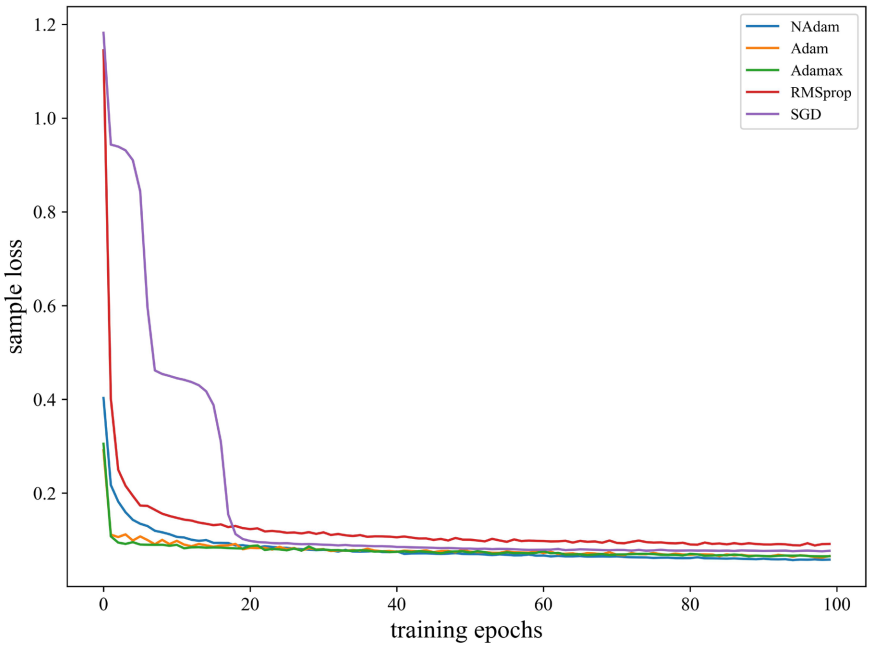

Figure 7. Training loss curves for different optimizers.

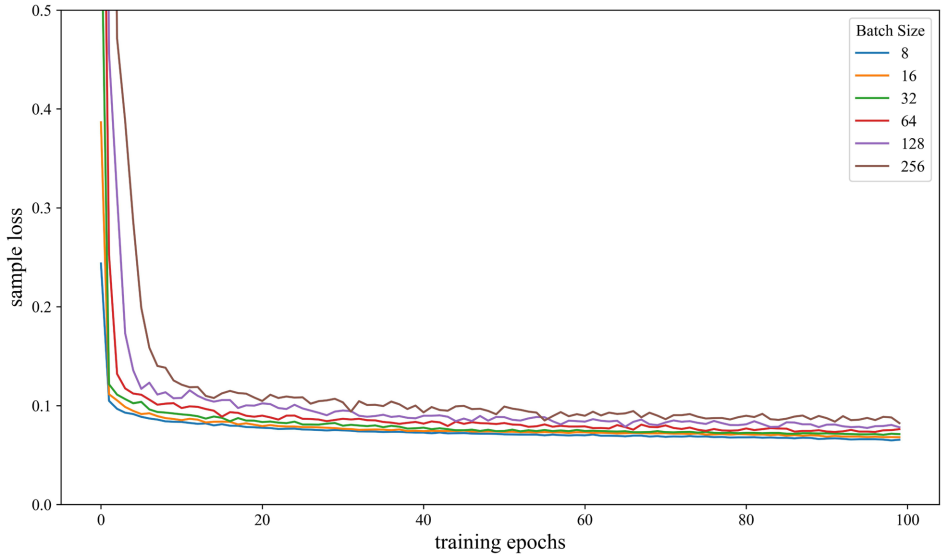

Figure 8. Training loss curves for different batch sizes.

The influence of different batch sizes on model performance is analyzed. A larger batch size can significantly improve computational efficiency. However, an overlarge batch size may lead to degraded generalization ability of the model and may also slow down the convergence speed during the learning process. Conversely, an excessively small batch size results in overly long training time and reduces overall efficiency. As shown in Figure 8, when the batch size is set to 16, the model achieves the best performance in terms of convergence speed and stability. Therefore, a batch size of 16 is selected for the proposed model.

Then, the influence of different numbers of hidden neurons on model perfor-

mance is analyzed. An excessive number of hidden neurons leads to an overly complex model and is prone to overfitting. Meanwhile, it also significantly increases the computational burden and reduces the training speed. On the contrary, an insufficient number of hidden neurons results in inadequate model capacity, which cannot effectively capture the complex features in the data, thus causing underfitting. As a result, the model fails to learn sufficient patterns from the training data, and the prediction accuracy decreases. As shown in Figure 9, when the number of hidden neurons is set to 64, the model not only converges rapidly but also effectively avoids overfitting. Therefore, the number of hidden neurons is set to 64 in the proposed model.

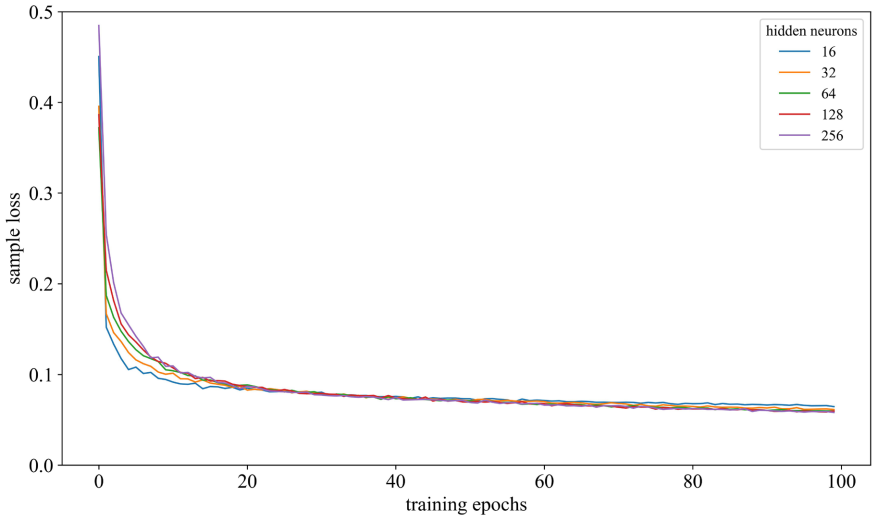

Figure 9. Training loss curve with different number of hidden neurons.

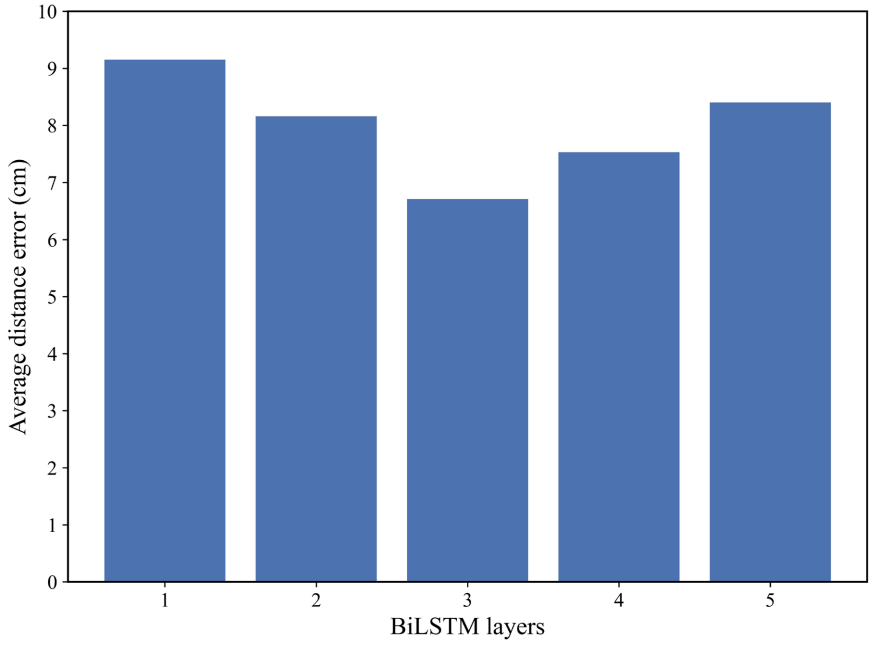

Figure 10. The average distance error of different BIGRU layers.

Finally, the influence of different network layers on model performance is analyzed. Figure 10 shows the average positioning distance error of the model under different numbers of BiLSTM layers. It can be observed from Figure 10 that the average positioning error decreases with the increase in the number of BiLSTM layers, leading to improved model performance. However, when the number of layers increases to 4 or more, the average positioning error begins to rise, resulting in degraded model performance. Accordingly, the proposed model adopts 3 BiLSTM layers.

The root mean square error (RMSE) loss function is chosen as the loss function of the model. Therefore, based on the training results obtained by adjusting different parameters, the values of each selected parameter in this paper are listed in Table 1.

After determining the optimal parameters, the parameters shown in Table 1 are used to verify the performance of the model on the test set. The average positioning error A (the total error of the model on the test set divided by the number of samples in the test set) is adopted to evaluate the prediction performance of the model.

$$A = \frac{1}{n}\sum_{i=1}^{n}\left(\left(x_i^{\text{true}} - x_i^{est}\right)^2 + \left(y_i^{\text{true}} - y_i^{est}\right)^2\right)^{0.5} \tag{21}$$

In the formula, $\left(x_i^{\text{true}}, y_i^{\text{true}}\right)$ denotes the true coordinate position of the UWB tag, and $\left(x_i^{est}, y_i^{est}\right)$ represents the estimated position predicted by the model. N denotes the total number of samples used for evaluation, which is 640 in the experiment.

Through multiple training runs of the model and calculation of the average error on the test set, the average error of the trained model on the test set is obtained as 6.7 cm.

Table 1. Detailed parameters of the convolutional layer.

BiLSTM Network Parameter	Value
Number of samples	3200
Ratio of training samples to total samples	0.8
Fixed number of training rounds	100
Batch size	16
Number of hidden neurons	64
Optimizer	NAdam
Learning rate	0.01
Number of LSTM layers	3
Loss function	RMSE

4.2. Comparison of Different Algorithms

Table 2 summarizes the training duration and test sample inference time for each

model in the UWB indoor positioning task. Both training time and inference time are based on the complete experimental process and are calculated as the average over multiple runs to ensure the reliability and reproducibility of the results. A comprehensive evaluation of model performance confirms the effectiveness of the proposed method.

It can be seen that the training time of the BiLSTM-Bahdanau model is significantly longer than that of traditional models such as RNN, LSTM and GRU. The main reason lies in the increased complexity of the model structure. On the one hand, BiLSTM adopts a bidirectional temporal modeling structure containing two independent LSTM units in forward and backward directions. During training, it needs to process both forward and backward dependencies of the sequence simultaneously, so the computational cost of forward propagation and backward gradient update is doubled. On the other hand, the Bahdanau attention mechanism dynamically calculates attention alignment weights for each time step during training, involving sequence similarity calculation, weight normalization and other additional operations not included in traditional RNNs, which further increases the computational complexity in the training phase and eventually leads to a substantial increase in training time.

In the inference phase, the inference time of the model for test samples is basically the same as that of other models, without introducing obvious additional time cost. The key reason is the essential difference between training and inference computation logic. First, the inference phase only performs a single forward propagation without backward gradient update and parameter iteration required in training, so the computational overhead of the bidirectional structure is greatly reduced in single inference without cumulative time cost. Second, the Bahdanau attention layer only calculates attention weights once based on fixed trained parameters during inference, with very small computation and little impact on the time cost of a single test sample. The test inference time of the model is 0.06 s, which has little impact on the real-time performance of the UWB positioning system.

Table 2. Training and prediction times of different recurrent neural networks.

Model	Training Time/s	Inference Time/s	Positioning Error/cm
RNN	9.38	0.05	11.3
LSTM	11.05	0.06	10.66
GRU	10.26	0.06	10.77
BiLSTM-Bahdanau	47.35	0.06	**6.7**

Overall, although the time cost in the training phase is increased, model training is an offline one-time operation for UWB positioning systems, and the time overhead is within the engineering acceptable range. In contrast, the inference phase serves as the online real-time positioning module. With negligible additional time cost, it achieves a significant improvement in positioning accuracy,

showing more practically valuable performance advantages in the trade-off between accuracy and efficiency.

Experimental results demonstrate that the proposed BiLSTM-Bahdanau model exhibits superior performance in UWB indoor positioning tasks compared with traditional recurrent neural network models such as RNN. Quantitatively, the average positioning error of this model is only 6.7 cm. Compared with the RNN, LSTM, and GRU models, the positioning error is reduced by approximately 40.71%, 37.15%, and 37.79%, respectively. These results strongly verify the effectiveness of the proposed method in improving UWB indoor positioning accuracy, which can provide a more solid technical support for high-precision positioning requirements in indoor scenarios.

5. Conclusions

In this study, the BiLSTM model combined with the Bahdanau attention mechanism is applied to UWB indoor positioning, and a novel indoor positioning method is proposed. This method takes the Time of Arrival (TOA) from the positioning tag to the base stations as the network input. The influences of different parameters on model performance are systematically analyzed from six aspects: learning rate, optimizer, batch size, number of network layers, number of hidden neurons, and loss function, and the optimal parameter configuration of the model is determined.

Experimental results show that the application of the BiLSTM model integrated with the Bahdanau attention mechanism in UWB indoor positioning achieves remarkable performance. Compared with other recurrent neural network models, the positioning error of the proposed model is significantly reduced. This indicates that with the continuous development of deep learning technology, neural networks combined with attention mechanisms will exhibit more prominent advantages in robustness and accuracy in complex environments, and their applications in the field of indoor positioning will be more extensive and in-depth in the future.

Conflicts of Interest

The authors declare no conflicts of interest regarding the publication of this paper.

References

[1] Elsanhoury, M., Makela, P., Koljonen, J., Valisuo, P., Shamsuzzoha, A., Mantere, T., *et al.* (2022) Precision Positioning for Smart Logistics Using Ultra-Wideband Technology-Based Indoor Navigation: A Review. *IEEE Access*, **10**, 44413-44445. https://doi.org/10.1109/access.2022.3169267

[2] Deng, W., Li, J., Tang, Y. and Zhang, X. (2023) Low-Complexity Joint Angle of Arrival and Time of Arrival Estimation of Multipath Signal in UWB System. *Sensors*, **23**, Article 6363. https://doi.org/10.3390/s23146363

[3] Huang, S., Chen, C., Wei, T., Tsai, W., Liou, C., Mao, Y., *et al.* (2023) Range-Extension Algorithms and Strategies for TDOA Ultra-Wideband Positioning System. *Sensors*,

23, Article 3088. https://doi.org/10.3390/s23063088

[4] Zhong, C., Lin, R., Zhu, H., Lin, Y., Zheng, X., Zhu, L., *et al.* (2024) UWB-Based AOA Indoor Position-Tracking System and Data Processing Algorithm. *IEEE Sensors Journal*, **24**, 30522-30529. https://doi.org/10.1109/jsen.2024.3442192

[5] Wang, F., Tang, H. and Chen, J. (2023) Survey on NLOS Identification and Error Mitigation for UWB Indoor Positioning. *Electronics*, **12**, Article 1678. https://doi.org/10.3390/electronics12071678

[6] Benouakta, A., Ferrero, F., Lizzi, L. and Staraj, R. (2023) Antenna Characteristics Contributions to the Improvement of UWB Real-Time Locating Systems' Reading Range and Multipath Mitigation. *IEEE Access*, **11**, 71449-71458. https://doi.org/10.1109/access.2023.3294622

[7] Kathikeyan, V. and Balamurugan, K. (2024) Underwater Multiple Access Communication Using Spread Spectrum Scheme. *National Academy Science Letters*, **49**, 211-215. https://doi.org/10.1007/s40009-024-01589-9

[8] Senevirathna, N.M., De Silva, O., Mann, G.K.I. and Gosine, R.G. (2022) Asymptotic Gradient Clock Synchronization in Wireless Sensor Networks for UWB Localization. *IEEE Sensors Journal*, **22**, 24578-24592. https://doi.org/10.1109/jsen.2022.3213696

[9] Qiao, J., Yang, F., Liu, J., Huang, G., Zhang, W. and Li, M. (2024) Advancements in Indoor Precision Positioning: A Comprehensive Survey of UWB and Wi-Fi RTT Positioning Technologies. *Network*, **4**, 545-566. https://doi.org/10.3390/network4040027

[10] Khan, I., Peralta, D., Fontaine, J., Soster de Carvalho, P., Martos Martinez-Caja, A., Antonissen, G., *et al.* (2025) Monitoring Welfare of Individual Broiler Chickens Using Ultra-Wideband and Inertial Measurement Unit Wearables. *Sensors*, **25**, Article 811. https://doi.org/10.3390/s25030811

[11] Li, X., Wang, H., Chen, Z., Jiang, Z. and Luo, J. (2024) UWB-Fi: Pushing Wi-Fi towards Ultra-Wideband for Fine-Granularity Sensing. *Proceedings of the* 22*nd Annual International Conference on Mobile Systems, Applications and Services*, Minato-ku, 3-7 June 2024, 42-55. https://doi.org/10.1145/3643832.3661889

[12] Jiang, R., Tang, L., Wang, X., Zhang, L., Xu, Y. and Li, D. (2024) An Adaptive Kalman Filter Combination Positioning Method Integrating UWB and GPS. *IEEE Transactions on Vehicular Technology*, **73**, 18222-18236. https://doi.org/10.1109/tvt.2024.3436851

[13] Guo, X., Ansari, N., Hu, F., Shao, Y., Elikplim, N.R. and Li, L. (2020) A Survey on Fusion-Based Indoor Positioning. *IEEE Communications Surveys & Tutorials*, **22**, 566-594. https://doi.org/10.1109/comst.2019.2951036

[14] Olejniczak, A., Blaszkiewicz, O., Cwalina, K.K., Rajchowski, P. and Sadowski, J. (2020) Deep Learning Approach for LOS and NLOS Identification in the Indoor Environment. 2020 *Baltic URSI Symposium* (*URSI*), Warsaw, 5-8 October 2020, 104-107. https://doi.org/10.23919/ursi48707.2020.9253757

[15] Tan Anh Nguyen, D., Lee, H., Joung, J. and Jeong, E. (2020) Convolutional Neural Network-Based UWB System Localization. 2020 *International Conference on Information and Communication Technology Convergence* (*ICTC*), Jeju, 21-23 October 2020, 488-490. https://doi.org/10.1109/ictc49870.2020.9289326

[16] Poulose, A. and Han, D.S. (2020) UWB Indoor Localization Using Deep Learning LSTM Networks. *Applied Sciences*, **10**, Article 6290. https://doi.org/10.3390/app10186290

[17] He, S., Yang, B., Liu, T. and Zhang, H. (2024) Multi-Tag UWB Localization with Spatial-Temporal Attention Graph Neural Network. *IEEE Transactions on Instrumentation and Measurement*, **73**, 1-12. https://doi.org/10.1109/tim.2024.3462984

[18] He, X., Mo, L. and Wang, Q. (2023) An Attention-Assisted UWB Ranging Error

Compensation Algorithm. *IEEE Wireless Communications Letters*, **12**, 421-425. https://doi.org/10.1109/lwc.2022.3229104

[19] Poulose, A., Kim, J. and Han, D.S. (2019) A Sensor Fusion Framework for Indoor Localization Using Smartphone Sensors and Wi-Fi RSSI Measurements. *Applied Sciences*, **9**, Article 4379. https://doi.org/10.3390/app9204379

[20] Raza, U., Khan, A., Kou, R., Farnham, T., Premalal, T., Stanoev, A., *et al.* (2019) Dataset: Indoor Localization with Narrow-Band, Ultra-Wideband, and Motion Capture Systems. *Proceedings of the* 2*nd Workshop on Data Acquisition to Analysis*, New York, 10 November 2019, 34-36. https://doi.org/10.1145/3359427.3361919